

Revival of Classical Vortex Generators Now for Transition Delay

Shahab Shahinfar,¹ Sohrab S. Sattarzadeh,¹ Jens H. M. Fransson,¹ and Alessandro Talamelli^{1,2}

¹Linné Flow Centre, KTH Mechanics, SE-10044 Stockholm, Sweden

²DIEM, Alma Mater Studiorum—Università di Bologna, I-47100 Forlì, Italy

(Received 23 April 2012; published 16 August 2012)

Classical vortex generators, known for their efficiency in delaying or even inhibiting boundary layer separation, are here shown to be coveted devices for transition to turbulence delay. The present devices are miniature with respect to classical vortex generators but are tremendously powerful in modulating the laminar boundary layer in the direction orthogonal to the base flow and parallel to the surface. The modulation generates an additional term in the perturbation energy equation, which counteracts the wall-normal production term and, hence, stabilizes the flow. Our experimental results show that these devices are really effective in delaying transition, but we also reveal their Achilles' heel.

DOI: [10.1103/PhysRevLett.109.074501](https://doi.org/10.1103/PhysRevLett.109.074501)

PACS numbers: 47.85.lf, 47.20.Pc, 47.27.Cn, 47.85.lb

When considering the flow over a surface, a boundary layer is developed due to the fluid viscosity with the disadvantage to bring about skin-friction drag, often quantified by its skin-friction coefficient c_f . Depending on the Reynolds number (Re), the surface roughness, and the external disturbance level, the flow will either be laminar or turbulent. For a given free-stream velocity, U_∞ , it is the boundary layer scale δ that determines the value of $Re(= \delta U_\infty / \nu = \sqrt{x U_\infty / \nu})$ or, alternatively, the downstream distance from the leading edge (x). Here ν is the kinematic viscosity.

The transition process from laminar to turbulent flow is not unique (see, e.g., the review in Ref. [1]), and today there are at least two representations of the evolution of small amplitude disturbances when testing the stability of base flows, namely the modal and the nonmodal approach. The former is characterized by exponentially growing (or decaying) disturbances for a certain range of forcing frequencies and Re numbers, and the first unstable eigenmode is the so-called Tollmien-Schlichting (TS) wave [2–4]. The latter is the transient disturbance growth characterized by an algebraic growth of an initial perturbation, often calculated iteratively as an optimal perturbation, which is followed by an algebraic viscous decay [5,6]. The initial perturbation is three-dimensional (3D) and optimized in the sense that it produces maximum growth at a certain downstream distance (or time). Due to the non-normality of the governing differential operator [7], the disturbance energy starts to grow at a subcritical Re, when compared with the modal approach, and if the disturbance reaches high enough amplitude, it will transition to turbulence in a bypass sense [8], since it completely bypasses the modal growth description. The study of transient growth is of fundamental interest since this type of instability appears in numerous applications, involving disturbance growth not only in canonical shear flows but also in areas such as lasers, ionospheric dynamics, magnetohydrodynamics, plasma physics, granular flow dynamics, and thermocapillary driven spreading, just to mention a few.

A laminar boundary layer has a relatively low skin-friction drag with respect to a turbulent one, and for increasing Re the difference in c_f rapidly increases. In many industrial applications, the difference can easily amount to an order of magnitude. This explains why there is a tremendous interest in being able to delay transition to turbulence, particularly by means of a passive mechanism, which has the advantage of accomplishing the control without adding any extra energy into the system. Moreover, a passive control does not have to rely on typically complicated sensitive electronics in sensor-actuator systems. This has been an endeavor by Fransson and coworkers [9–11] who made use of circular roughness elements, positioned on a flat plate, in order to generate streamwise streaks, i.e., regions with alternating high and low fluid velocity in the direction orthogonal to the base flow. To our knowledge the first successful experimental study on TS wave stabilization using steady streamwise streaks was reported in [12]. Unsteady streaks generated by means of free-stream turbulence have also been shown to act stabilizing on both TS waves and the spreading of turbulent spots [13,14]. It should, however, be pointed out that none of them, except [11], has successfully shown transition delay. More recently, this has also been confirmed by means of large-eddy simulations [15].

In an attempt to show that this passive flow control method will work in real flow applications, we must prove that bypass transition is not activated by (i) the instability of the streaks or (ii) the receptivity of an incoming TS wave by the roughness array. The threshold streak amplitude prior to breakdown to turbulence using circular roughness elements was found to be 12% of U_∞ [9]. The hypothesis, confirmed in [10], was that the higher the streak amplitude is for a fixed spacing between individual roughness elements, the greater the stabilizing effect. Therefore, in order to increase this value, a new set of devices was designed, namely miniature vortex generators (MVGs), which were tested for natural bypass transition without forced disturbances [16]. The MVG design was

based on a pseudoviscous vortex model [17]. It was shown that steady laminar streamwise streaks may be generated in a low disturbance wind tunnel, using MVGs, with an amplitude up to 32% of U_∞ before the onset of bypass transition. Furthermore, the increase in the local skin-friction drag was quantified, by using the von Kármán integral equation, to about 12% right behind the MVG array for a streaky base flow with an amplitude of 25% of U_∞ . This increase is judged to be small if compared to the advantage of keeping the boundary layer laminar with c_f -values, typically, one order of magnitude smaller than the corresponding turbulent ones.

The purpose of the present experimental investigation is to test the effectiveness of MVGs to stabilize TS waves in a realistic flow configuration with the aim to obtain transition delay in flat plate boundary layers. This type of passive control idea is really appealing and worthy of being pushed to its limit.

The experiments were performed in the low speed closed circuit minimum-turbulence-level wind tunnel at the Royal Institute of Technology (KTH) in Stockholm. The tunnel is renowned for its high flow quality (low background disturbance level and high flow homogeneity) and is well suited for stability experiments [18]. Phase-triggered single hot-wire anemometry has been used as measurement technique due to its good accuracy and resolution. This is a single point measurement technique where the sampling frequency (temporal resolution) is set by the user, typically 20 kHz without any problem, and where the spatial resolution is given by the length of the hot-wire probe, which here was 0.5 mm.

In Fig. 1 a sketch of the flat plate is shown and where the coordinate system (x, y, z) is introduced with the corresponding velocity components (U, V, W) , small letters denote perturbations. Here, the flow domain can be divided into four regions. In region (I) a two-dimensional (2D) laminar boundary layer develops on the flat plate, while in (II) TS waves are generated by means of blowing and suction through a spanwise slot in the plate located at x_{TS} . The unsteady blowing and suction is created by a sealed loudspeaker connected to the slot via vinyl hoses (as described in [10]). The loudspeaker is driven by a computer generated sinusoidal output signal via an amplifier and the measurements are triggered based on the phase of this output signal. Throughout this Letter, we use the non-dimensional frequency $F = (2\pi f\nu/U_\infty^2) \times 10^6$, where f Hz is the forcing frequency. For the present MVG configuration $F \approx 102, 135, 178$ were tested. In region (III) the 3D streaky base flow with alternating high and low speed streaks are generated by the MVG array located at x_{MVG} . The distance between neighboring MVG pairs is $\Lambda = 13$ mm. In this investigation we have considered three different MVG heights $h = 1.1, 1.3, \text{ and } 1.5$ mm, giving rise to successively intensified vortices provided that U_∞ is kept constant, which in turn results in stronger modulations of the originally 2D base flow. In region (IV)

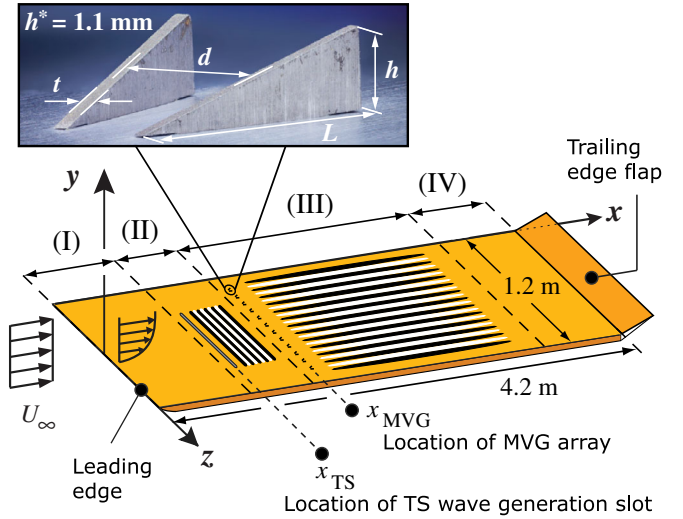


FIG. 1 (color online). Schematic of the flat plate boundary layer with the (I–IV) regions described in the text. The black and white striped pattern perpendicular to the main stream, downstream of the disturbance slot in region (II), indicates the TS waves. In region (III) a similar striped pattern aligned with the main stream indicates the alternating high and low speed streaks. Inset shows a photo by John Hallmén of a MVG pair. $x_{TS} = 190$ mm and $x_{MVG} = 222$ mm from the leading edge. $h = 1.1, 1.3, 1.5$, $L = d = 3.25$, and $t = 0.3$ (mm).

the amplitude of the streaky base flow has finally decayed and the 2D base flow found in region (I) will eventually be recovered, unless the streaks breakdown to turbulence.

In tracing the amplitude growth of TS waves in the streaky base flow in the downstream direction and from there make adequate comparisons with the 2D reference case, it is necessary to define an integral TS wave amplitude measure over the cross-sectional yz plane, based on the local TS amplitude $A_{TS}(x, y, z)$. Here we integrate over one period of the streaky base flow in the spanwise direction and in the wall-normal direction up to some truncated distance η^* (here equal to 9) according to

$$A_{TS}^{yz}(x) = \int_{-1/2}^{1/2} \int_0^{\eta^*} \frac{A_{TS}(x, y, z)}{U_\infty} d\eta d\zeta, \quad (1)$$

where $\eta = y/\delta$ and $\zeta = z/\Lambda$. For the 2D reference base flow, the TS wave distribution is close to homogeneous in the spanwise direction (the standard deviation in the z direction of the wall-normal TS wave amplitude distribution was typically 0.3% of U_∞), and hence only the wall-normal integral was evaluated. In order to quantify the influence of the streaky base flow amplitude we need an amplitude measure, which we here define as

$$A_{ST}(x) = \max_y \{\Delta U(y)/2\} / U_\infty,$$

$$\text{where } \Delta U(y) = \max_z \{U(y, z)\} - \min_z \{U(y, z)\}. \quad (2)$$

Note that as long as Λ is unchanged, the above definition is sufficient, i.e., no need to define an integral measure of the

streaky base flow amplitude. These measures have previously been used in this type of 3D streaky boundary layers, see [10], which facilitates comparisons. Figure 2 gives an idea of how the mean streaky base flow of the streamwise velocity component 2(a) and the TS wave amplitude distribution $A_{TS}(x, y, z)$ (for $F = 178$) 2(b) look like in the cross-sectional plane for a particular downstream location behind the MVGs. This type of cross-sectional planes have been produced based on 20×14 measurement points in the yz plane. Figure 2(a) shows the modulated base flow with a high speed region in the center of the figure and low speed regions on the sides, being produced by the strong counter-rotating vortices set up by an MVG pair, which bring high speed fluid downwards on the center line and lifts low speed fluid from the wall on the sides (see Ref. [16]).

In Fig. 3 the streak amplitude [Eq. (2)] and the TS amplitude [Eq. (1)] growth curves are shown in Figs. 3(a) and 3(b), respectively, for successively increasing h . Here the TS wave growth curves in 3(b) have been normalized with the amplitude measured closest to the MVG array ($A_{TS,0}^{yz}$), this in order to fairly show the amplitude response of the TS wave passing the MVG array. The maximum streak amplitudes are 17, 21, and 28% of U_∞ for $h = 1.1, 1.3, 1.5$ mm, respectively.

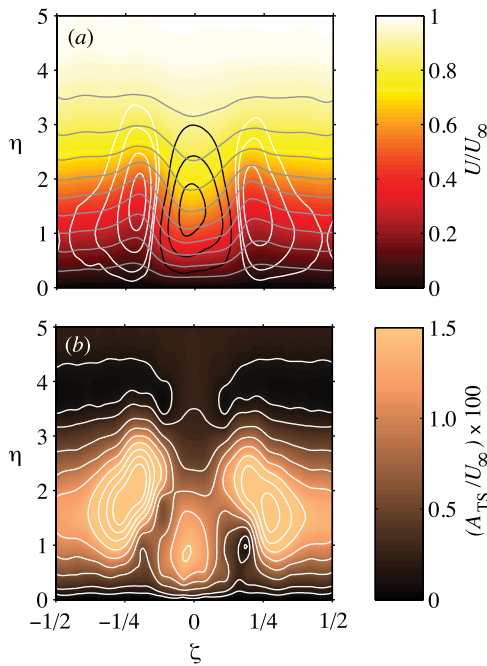


FIG. 2 (color online). (a) Three-dimensional base flow modulation with solid white and black contour lines corresponding to regions of velocity deficit and excess, respectively, with respect to the 2D base flow. Solid gray contour lines represent lines of constant velocity from $U/U_\infty = 0.1$ to 0.9 with an increment of 0.1 . (b) Amplitude distribution of a TS wave with $F = 178$ in the base flow shown in (a). The white contour lines correspond to constant TS wave amplitudes. $U_\infty = 6.0 \text{ m s}^{-1}$ and $(x - x_{\text{MVG}})/h = 33$. $\zeta = 0$ correspond to the center line of a MVG pair. $h = 1.3 \text{ mm}$.

1.3, 1.5 mm, respectively. The physical mechanism behind the stabilization (reduced growth), as observed in 3(b) for increasing h from 0 to 1.3 mm beyond $\text{Re} \approx 460$, can be understood by looking at the perturbation energy equation. In the modulated case there is indeed an extra production term, namely the Reynolds stress $-\overline{uw}$ acting on $\partial U/\partial z$, in addition to the wall-normal production term $-\overline{uv}\partial U/\partial y$. The former term turns out to be of negative sign and can, together with the viscous dissipation, quench the wall-normal positive production term [19]. In Fig. 3(b), one may conclude that for the highest amplitude case (circles; $h = 1.5 \text{ mm}$), the boundary layer bypasses to transition and the stabilizing effect of the TS wave fails to come off; instead, the relative TS wave amplification is about a factor of three ($> e^1$) higher compared to the reference case at around $\text{Re} = 600$. In 3(a) it is shown that the streak amplitude decays remarkably fast after $\text{Re} = 550$ due to turbulence/transitional mixing. On the other hand, for the intermediate streak amplitude case (triangles) in 3(b), the TS wave is strongly damped and decays exponentially after some initial growth caused by a complex receptivity of the wave by the MVG array. This initial growth, with a maximum around $\text{Re} = 400$, increases with h and the maximum TS amplitude in 3(b) seems to correspond to the streamwise location of maximum streak amplitude in 3(a). From the data in 3(b), it is clear that the change of the TS growth curve in the 2D reference base flow (stars)

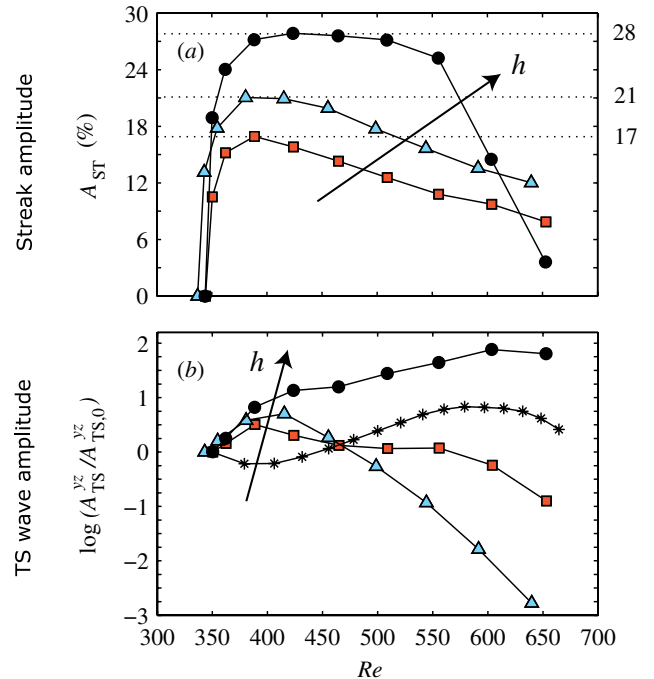


FIG. 3 (color online). (a) Streak amplitude (A_{ST}) and (b) TS wave amplitude (A_{TS}^{yz}) distribution in the downstream direction for constant $U_\infty \approx 7.8 \text{ m s}^{-1}$ and $F \approx 135$. The different symbols (squares, triangles, circles) correspond to different MVG heights $h = 1.1, 1.3, 1.5 \text{ mm}$, respectively. Stars in (b) correspond to the 2D base flow case without MVGs.

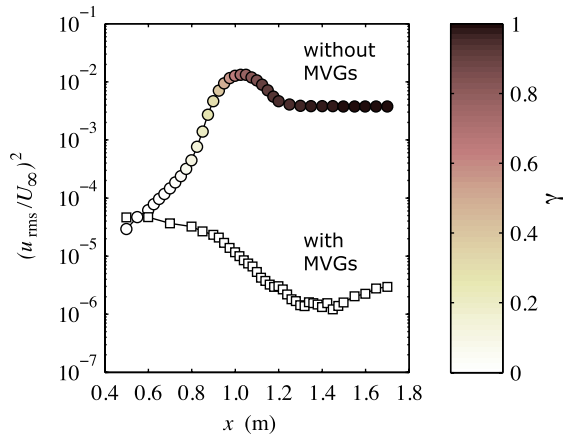


FIG. 4 (color online). Energy evolution in the downstream direction with and without MVGs plotted with squares and circles, respectively, at $U_\infty = 7.7 \text{ m s}^{-1}$. The same high initial forcing amplitude and frequency ($F = 102$) of the TS wave were applied. MVGs: $h = 1.3 \text{ mm}$ giving a maximum A_{ST} of 21%. The color bar applied on the symbols corresponds to the intermittency (γ) of the velocity signal.

is gradual for increasing h . For the smallest h (squares), one may get an inkling of a plateau region around $\text{Re} = 500\text{--}550$, even though the relative growth has been reduced. This trend is in agreement with previous results on TS wave growth curves in streaky boundary layers generated by means of circular roughness elements, but when introduced in an already developed streaky boundary layer [10]. Same conclusions may be drawn for all three tested TS wave frequencies.

Having encountered an initial growth of the TS wave amplitude due to a hitherto unknown receptivity mechanism by the MVG array it is not trivial that the aim of accomplishing transition delay would be met. Figure 4 shows one case of constant high initial amplitude forcing of a TS wave at $F = 102$ with and without the MVG array. The color bar represents the intermittency of the velocity signal (γ), which here is a statistical measure of the proportion of laminar versus turbulent flow sweeping the hot-wire probe. For $x \geq 1.2 \text{ m}$ the velocity signal acquired without the presence of MVGs is completely turbulent with a γ -value close to unity. With the MVGs mounted a complete nullification of the disturbance growth is shown (see Fig. 4). The streaky base flow continuously acts stabilizing in the streamwise direction rendering the streamwise disturbance amplitude (u_{rms}) to levels below 0.14% of U_∞ inside the boundary layer. The velocity signal was acquired at a wall-normal distance corresponding to the displacement thickness of the boundary layer, which is the location where the inner amplitude peak of a TS wave typically is encountered. Here we apply a high-pass filter, with a cutoff frequency of $F_{\text{cut}} \approx 30$, prior to the calculation of the root-mean-square value of the streamwise velocity signal. Similar results of transition delay were also obtained for $F = 135$ and 178.

A simple estimation of the skin-friction drag reduction based on standard empirical relations of laminar and turbulent boundary layers, only considering the interval $6.2 \times 10^5 \leq \text{Re}_x \leq 8.7 \times 10^5$ (i.e., $1.2 \leq x \leq 1.7 \text{ m}$), amounts to a value of 22%. This figure represents the lower limit of the drag reduction observed in Fig. 4, which is promising, considering that (1) one could probably have measured even further downstream with the present MVGs and have been able to improve the estimated figure, (2) the MVG devices have not yet been optimized, and (3) a second array of MVGs in order to regenerate the streaky base flow and, in turn, reinforce the stabilizing effect on the boundary layer has not been tested yet (see Ref. [16]).

In this experimental investigation, we show that miniature classical vortex generators are really suitable devices in accomplishing transition delay and plausible to work in real flow applications. MVGs are clearly superior to circular roughness elements, since the flow is allowed to pass right through them, possibly reducing the absolute instability region behind the devices and allowing for twice as high amplitude streaks to be generated, but still with some margin to the threshold amplitude beyond which the streaky base flow becomes unstable. This makes the streaky base flow much more robust for external perturbations, a prerequisite for real flow applications. Furthermore, in the present setup the TS waves are being generated upstream of the MVG array, leaving the full and nasty receptivity process of the incoming wave by the MVG array, which really challenges the present passive flow control method. Despite the initial growth of the TS wave amplitude behind the MVG array transition delay is convincingly accomplished as long as the streak amplitude stays below some threshold amplitude (around 25%). Beyond this threshold amplitude, the boundary layer bypasses to transition and the passive flow control technique not only fails, but it advances transition and, hence, increases the skin-friction drag, which may be seen as the Achilles' heel of the MVG devices. The present result shows the first convincing transition delay experiment in a realistic flow configuration using passive laminar flow control and is believed to encourage future works in the area.

J. H. M. F. acknowledges the European Research Council for its financial support of the AFRODITE project through a Starting Independent Researcher Grant.

-
- [1] Y. S. Kachanov, *Annu. Rev. Fluid Mech.* **26**, 411 (1994).
 - [2] W. Tollmien, *Nachrichten von der Gesellschaft der Wissenschaften zu Göttingen* **21** (1929) [National Advisory Committee for Aeronautics, Technical Memorandum 609, 1931].
 - [3] H. Schlichting, *Z. Angew. Math. Mech.* **13**, 260 (1933).
 - [4] G. B. Schubauer and H. K. Skramstad, *J. Aeronaut. Sci.* **14**, 69 (1947).
 - [5] P. Luchini, *J. Fluid Mech.* **327**, 101 (1996).
 - [6] P. Luchini, *J. Fluid Mech.* **404**, 289 (2000).

- [7] L.N. Trefethen, A.E. Trefethen, S.C. Reddy, and T.A. Driscoll, *Science* **261**, 578 (1993).
- [8] M.V. Morkovin, in *Viscous Drag Reduction*, edited by C.S. Wells (Plenum, New York, 1969).
- [9] J.H.M. Fransson, L. Brandt, A. Talamelli, and C. Cossu, *Phys. Fluids* **16**, 3627 (2004).
- [10] J.H.M. Fransson, L. Brandt, A. Talamelli, and C. Cossu, *Phys. Fluids* **17**, 054110 (2005).
- [11] J.H.M. Fransson, A. Talamelli, L. Brandt, and C. Cossu, *Phys. Rev. Lett.* **96**, 064501 (2006).
- [12] Y.S. Kachanov and O.I. Tararykin, *Izvestiya Sibirskogo Otdeleniya Akademii Nauk SSSR, Seriya Khimicheskikh Nauk* **18** (1987).
- [13] K.J.A. Westin, A.V. Boiko, B.G.B. Klingmann, V.V. Kozlov, and P.H. Alfredsson, *J. Fluid Mech.* **281**, 193 (1994).
- [14] J.H.M. Fransson, *Phys. Rev. E* **81**, 035301(R) (2010).
- [15] P. Schlatter, E. Deusebio, R. de Lange, and L. Brandt, *Int. J. Flow Contr.* **2**, 259 (2010).
- [16] J.H.M. Fransson and A. Talamelli, *J. Fluid Mech.* **698**, 211 (2012).
- [17] O. Lögdberg, J.H.M. Fransson, and P.H. Alfredsson, *J. Fluid Mech.* **623**, 27 (2009).
- [18] B. Lindgren and A.V. Johansson, KTH Mechanics report KTH/MEK/TR02/13SE, 2002.
- [19] C. Cossu and L. Brandt, *Eur. J. Mech. B, Fluids* **23**, 815 (2004).